Z. Phys. D – Atoms, Molecules and Clusters 11, 105–111 (1989)

Atoms, Molecules
Zeitschrift für Physik D and Clusters

Quadrupole moments of radium isotopes from the $7p\,^2P_{3/2}$ hyperfine structure in Ra II

W. Neu[1]*, R. Neugart[1], E.-W. Otten[1], G. Passler[1], K. Wendt[1], B. Fricke[2] E. Arnold[3], H.J. Kluge[3], G. Ulm[3]***, and the ISOLDE Collaboration[3]**

[1] Institut für Physik, Universität Mainz, D-6500 Mainz, Federal Republic of Germany
[2] Fachbereich Physik, Gesamthochschule Kassel, D-3500 Kassel, Federal Republic of Germany
[3] CERN, CH-1211 Geneva, Switzerland

Received 1 September 1988

The hyperfine structure and isotope shift of $^{221-226}$Ra and ^{212,214}Ra have been measured in the ionic (Ra II) transition $7s\,^2S_{1/2}-7p\,^2P_{3/2}$ ($\lambda=381.4$ nm). The method of on-line collinear fast-beam laser spectroscopy has been applied using frequency-doubling of cw dye laser radiation in an external ring cavity. The magnetic hyperfine fields are compared with semi-empirical and ab initio calculations. The analysis of the quadrupole splitting by the same method yields the following, improved values of spectroscopic quadrupole moments: $Q_s(^{221}\text{Ra})=1.978(7)$b, $Q_s(^{223}\text{Ra})=1.254(3)$b and the reanalyzed values $Q_s(^{209}\text{Ra})=0.40(2)$b, $Q_s(^{211}\text{Ra})=0.48(2)$b, $Q_s(^{227}\text{Ra})=1.58(3)$b, $Q_s(^{229}\text{Ra})=3.09(4)$b with an additional scaling uncertainty of $\pm 5\%$. Furthermore, the J-dependence of the isotope shift is analyzed in both Ra II transitions connecting the $7s\,^2S_{1/2}$ ground state with the first excited doublet $7p\,^2P_{1/2}$ and $7p\,^2P_{3/2}$.

PACS: 31.30.G; 31.30.J; 35.10.F; 42.65.C

1. Introduction

Laser spectroscopy experiments have provided the first directly measured ground-state spins and a number of magnetic dipole and electric quadrupole interaction parameters from the hyperfine structure (hfs) of the odd-A radium ($Z=88$) isotopes [1, 2]. The magnetic moments μ_I and spectroscopic quadrupole moments Q_s were deduced from these parameters by a semi-empirical analysis of the magnetic hyperfine fields and electric field gradients. Recently, the direct observation of nuclear Larmor precession in ^{213}Ra and ^{225}Ra has yielded absolute g_I-values [3] and hence has offered the possibility of determining magnetic hyperfine fields from measured hfs coupling constants (A-factors). In the case of the $7s\,^2S_{1/2}$ ground state of Ra II the experimental result agrees within 2–4%, depending on the choice of the relativistic correction factors used, with a semi-empirical calculation of the hyperfine fields by means of the Goudsmit-Fermi-Segrè formula. The semi-empirical procedure thus proves to be reliable even for the high-Z elements such as radium. The accuracy is similar for large-scale ab initio calculations of the magnetic hyperfine field [4–6] using relativistic many-body perturbation theory (RMBPT).

The present work aims primarily at a more reliable determination of the spectroscopic quadrupole moments Q_s of the radium isotopes. The Q_s values given in [2] were based on a semi-empirical analysis of the hfs of the $7s\,7p\,^3P_J$ configuration in Ra I. This paper reports on the measurement and analysis of the hfs of the transition $7s\,^2S_{1/2}-7p\,^2P_{3/2}$ ($\lambda=381.4$ nm) in the alkali-like Ra II. The hyperfine splitting of the upper state is expected to give more reliable values for the spectroscopic quadrupole moments, because the calculation of the electric field gradient concerns only a single valence-electron configuration.

The additionally measured isotope shifts (IS) combined with those of the earlier investigated transition

* Present address: CERN, CH-1211 Geneva 23, Switzerland
** Present address: Institut für Physik, Universität Mainz, D-6500 Mainz, Federal Republic of Germany
*** Present address: Physikalisch-Technische Bundesanstalt, D-1000 Berlin 10, Germany

$7s\,^2S_{1/2} - 7p\,^2P_{1/2}$ allow the determination of the relativistically enhanced charge density of the $p_{1/2}$-electron at the position of the nucleus. This effect is appreciable because of the high Z-value of radium.

2. Experimental technique

As in previous experiments on the radium isotopes [1, 2, 7] we used collinear fast-beam laser spectroscopy at the ISOLDE facility at CERN. The measurements were performed on a selection of isotopes which are most abundantly produced by proton-induced spallation in a ThC_2 target. The yields of these isotopes, ^{212,214}Ra and $^{221-226}$Ra, range from $1.8 \cdot 10^7$ to $7 \cdot 10^9$ atoms per second for a 600 MeV proton current of 2 μA [8].

The setup in its different versions for spectroscopy on neutral atoms and ions and for ultraviolet (UV) detection has been described in [9–12]. In the present experiment we have introduced the UV excitation by frequency doubling of cw laser radiation, which will be described in some more detail.

The frequency-doubling system

The light source consists of a commercial tunable cw laser system and an external ring cavity for the frequency doubling. A single-mode ring dye laser is pumped by a krypton-ion laser and operated with the dye LD700. The dye-laser output is typically 600 mW at a wavelength of $\lambda = 762.8$ nm. The external cavity is actively locked into resonance by monitoring the frequency-dependent elliptical polarization of the light reflected from the cavity. The dispersion-shaped signal serves as a feedback to tune the length of the resonator with a piezo-mounted mirror. This stabilization scheme, developed by Hänsch and Couillaud [13], provides resonance enhancement by a factor of 40–50. The employed $LiIO_3$ frequency doubling crystal is placed inside this cavity. $LiIO_3$ is an uniaxial, highly birefringent optically active crystal. Its nonlinear coefficient exceeds those of the commonly used frequency-doubling crystals by more than one order of magnitude [14, 15]. The superiority of $LiIO_3$ has been shown in previous experiments at wavelengths between $\lambda = 293$ nm–308 nm [16] and for a slightly extended range of $\lambda = 293$ nm–310 nm by Renn et al. [17].

In order to avoid reflection losses inside the cavity, the $LiIO_3$ crystal is cut at the appropriate phase-matching angle Θ_m to be used at Brewster angle. A special crystal mounting support has been constructed to facilitate the necessary adjustments illustrated in Fig. 1. The crystal can be rotated on an axis normal to its surface (ω). This rotation allows an adjustment of the optical axis perpendicular to the polarization (type I) of the incoming laser beam, thus avoiding birefringence for the ground wave. The necessary phase matching between the ground wave and the produced second harmonic is then achieved by tilting the optical axis of the crystal with respect to the direction of propagation of the incident laser beam (critical angle tuning). The virtually reflected beam defines the tilting axis. In this way the Brewster angle condition is nearly undisturbed within a tuning range of $\pm 5°$. The position of the $LiIO_3$ crystal at a focal point of the ring cavity (beam diameter $\simeq 50$ μm) gives the highest possible power density of the ground wave but also a non-Gaussian beam profile. The produced UV light is extracted from the external resonator by means of a dichroic beam splitter, which reflects more than 95% of the UV while transmitting 98% of the ground wave. The dielectric coating of the beam splitter is designed to be used at the Brewster angle in order to minimize the reflection losses. With the $LiIO_3$ crystal and the beam splitter in place the remaining losses, both reflection and absorption, cause a drop of the resonance enhancement to about 12–15 which is only slightly reduced by tuning the crystal. Owing to the quadratic power dependence of the second harmonic, the cavity enhancement thus increases the UV by a factor of 150–220. A maximum UV power of 10 mW has been obtained at $\lambda = 381.4$ nm with 600 mW single-mode output power from the dye laser. The UV power remains stable during more than 30 h without the necessity for readjustments. The high UV power also allows

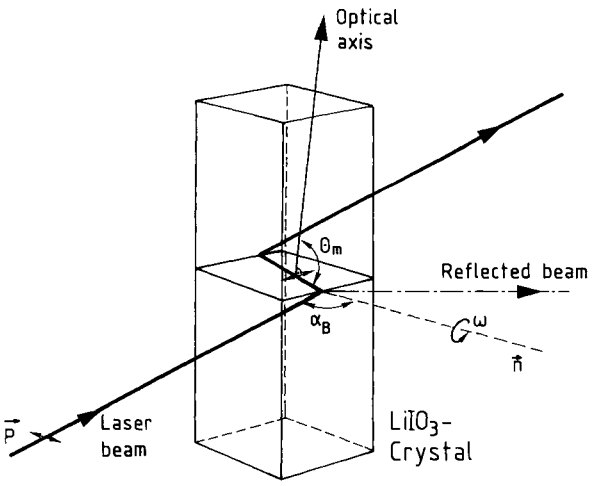

Fig. 1. The geometry of the $LiIO_3$ crystal. Θ_m: phase-matching angle. α: Brewster angle. $\vec{P}$: polarization of the incident laser beam. $\vec{n}$: axis normal to the crystal surface. ω: rotation around n

a shaping of the non-Gaussian beam profile by a diaphragm, to minimize the background produced by stray light from the laser.

3. The experimental data

The hfs of ^{221,223,225}Ra and the IS of the neutron-rich isotopes $^{221-226}$Ra relative to the reference isotopes ^{212}Ra and ^{214}Ra have been measured in the transition $7s\,^2S_{1/2}-7p\,^2P_{3/2}$ of Ra II. Figure 2 shows a typical spectrum of ^{221}Ra ($I=5/2$). The full width at half maximum of the fluorescence signals is about 40 MHz. The hyperfine constants A and B are fitted to the measured positions of the hyperfine levels by use of the formula for the hyperfine splitting energy [18]:

$$W_{\mathrm{hfs}}=\frac{1}{2}AC+\frac{3/4\,C(C+1)-J(J+1)\,I(I+1)}{2J(2J-1)\,I(2I-1)}B \qquad (1)$$

with

$$C=F(F+1)-J(J+1)-I(I+1)$$

where the total angular momentum is F, the angular momentum of the electron J, and the nuclear spin I. The A-factor is given by $A=\mu_I H_e(0)/(IJ)$, the product of the nuclear magnetic moment μ_I and the magnetic hyperfine field $H_e(0)$ of the electron core at the position of the nucleus. The electric quadrupole term, due to the electric field gradient of the electrons $\phi_{zz}(0)$ interacting with the nuclear quadrupole moment Q_s, is given by $B=eQ_s\,\phi_{zz}(0)\,(1-R)$, with $(1-R)$ being the Sternheimer correction factor [19]. The results for the investigated three odd-A isotopes are given in Table 1, together with the corresponding $A(^2P_{1/2})$-factors obtained earlier [1]. The IS values measured in this work are given in Table 2 and compared with previous results obtained in the transition $7s\,^2S_{1/2}-7p\,^2P_{1/2}$ [2]. All frequency differences are obtained by conversion from the voltage scale of

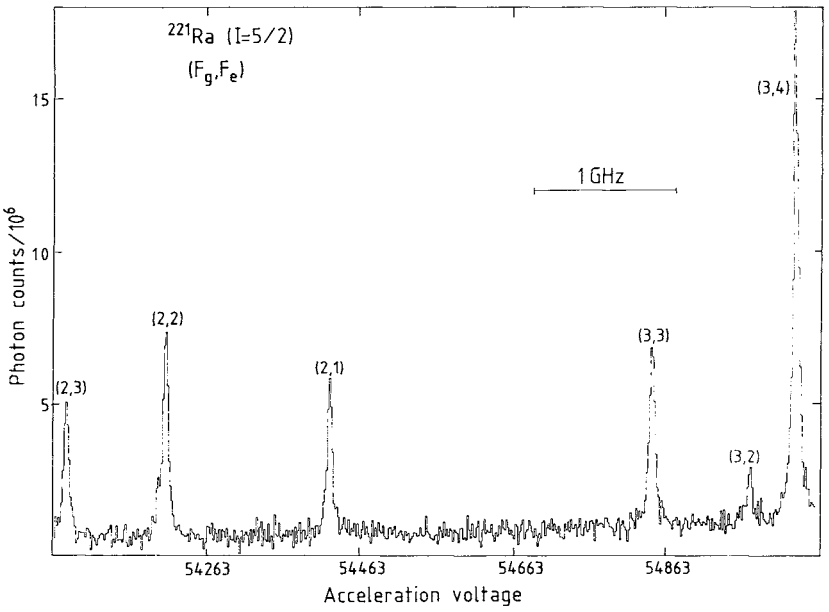

Fig. 2. Hyperfine structure of ^{221}Ra in the ionic transition $7s\,^2S_{1/2}-7p\,^2P_{3/2}$ at $\lambda=381.4$ nm obtained by Doppler-tuning

Table 1. Hyperfine constants A and B (given in MHz) of the transition $7s\,^2S_{1/2}-7p\,^2P_{3/2}(\lambda=381.4\,\mathrm{nm})$ in Ra II. The nuclear spins I [1], the magnetic moments μ_I [3] and the A-factors for the $^2P_{1/2}$-state in Ra II [2] are also included

A	I	$\mu_I(\mu_N)$	$A(^2S_{1/2})$	$A(^2P_{3/2})$	$B(^2P_{3/2})$	$A(^2P_{1/2})$
221	5/2	−0.179 (2)	− 1348.6 (1.8) − 1345.0 (1.8)[a]	− 22.4 (9)	1364.2 (5.1)	− 266.3 (1.5)[a]
223	3/2	0.271 (3)	3404.0 (1.9) 3398.3 (2.9)[a]	56.5 (8)	864.8 (1.9)	667.1 (2.1)[a]
225	1/2	−0.7348 (15)	−27731 (13) −27684 (13)[a]	−466.4 (4.6)		−5446 (7)[a]

[a] Taken from [2]; the discrepancies with the present values may be due a slight miscalibration of the Doppler-tuning

Table 2. Isotope shifts in the transition $7s\,^2S_{1/2}-7p\,^2P_{3/2}(\delta\nu_{381})$ compared to the values obtained in the transition $7s\,^2S_{1/2}-7p\,^2P_{1/2}(\delta\nu_{468})$ [2] of Ra II. The common reference isotope is ^{214}Ra

A	$\delta\nu_{381}$ (Mhz)	$\delta\nu_{468}$ (Mhz)
212	4937 (2)	4583 (3)
214	0	0
221	−39222 (18)	−36496 (14)
222	−43572 (14)	−40552 (14)
223	−49050 (18)	−45657 (16)
224	−53076 (21)	−49411 (16)
225	−58776 (22)	−54710 (18)
226	−62159 (21)	−57852 (18)

Doppler tuning. The errors are the sum of the systematic uncertainty in the measurement of the acceleration voltages (10^{-4}), which contributes an uncertainty of about 0.5 MHz per atomic mass unit for the isotope shifts (see [9]) and the statistical error as extracted from the χ^2 of the fitting procedure.

4. Analysis of the hfs in the $7p\,^2P_j$ configuration

4.1. Magnetic hyperfine fields

Following the relativistic effective operator formalism [20, 21] the A-factors are decomposed into an orbital (a_{01}), a spin dipolar (a_{12}), and a contact (a_{10}) term. For a p-electron one obtains

$$\begin{aligned} A(p_{1/2}) &= (4/3)\,a_{01}+(4/3)\,a_{12}-(1/3)\,a_{10} \\ &= a_{p_{1/2}}-(1/3)\,a_{10} \\ A(p_{3/2}) &= (2/3)\,a_{01}+(2/15)\,a_{12}-(1/3)\,a_{10} \\ &= a_{p_{3/2}}+(1/3)\,a_{10}. \end{aligned} \tag{2}$$

In the traditional theory the two first terms on the left hand side are contracted to the one-electron a_{nlj}-factors [18]

$$\begin{aligned} a_{nlj} &= \frac{(2\mu_0\,\mu_B)}{4\pi}\,\frac{\mu_I}{I}\,\frac{l(l+1)}{j(j+1)} \\ &\quad\cdot\langle r^{-3}\rangle_{nl}\,F_j(Z_i)\,(1-\delta)\,(1-\varepsilon), \end{aligned} \tag{3}$$

where $\langle r^{-3}\rangle_{nl}$ is the radial matrix element in the valence state (n, l), $F_j(Z_i)$ a relativistic correction factor, Z_i the effective nuclear charge, $(1-\varepsilon)$ the Bohr-Weisskopf and $(1-\delta)$ the Breit-Rosenthal-Schawlow volume correction. Schwartz [22] has calculated for p-electrons the ratio

$$\begin{aligned} \Theta &= (\langle r^{-3}\rangle_{np_{1/2}}\,F_{1/2})/(\langle r^{-3}\rangle_{np_{3/2}}\,F_{3/2}) \\ &= (N_{1/2}/N_{3/2})\,(F_{1/2}/F_{3/2}), \end{aligned} \tag{4}$$

which includes in addition to the ratio of the F_j a slight j-dependence of the normalization constant N_j for the wave function near the origin. With $\Theta(\mathrm{Ra})=2.51$, $(1-\delta)_{p_{1/2}}=0.95$, $(1-\varepsilon)_{p_{1/2}}=0.99$, and $\delta=\varepsilon=0$ for the $p_{3/2}$-electron one obtains for the ratio of the a_{nlj}-factors $a_{7p_{1/2}}/a_{7p_{3/2}}=11.8$. Inserting this ratio and the experimental A-factors into (2) results in

$$a_{10}(^{225}\mathrm{Ra}) = -13.5(12.9)\ \mathrm{MHz} \tag{5}$$

for the contact term of ^{225}Ra, which, within the error, is hardly different from zero. The two other less precisely measured isotopes yield no significant contact term. Reinserting (5) into (2) we obtain for further use:

$$\begin{aligned} a_{1/2} &= 1.001(1)\,A_{1/2} \\ a_{3/2} &= 0.99(1)\,A_{3/2}. \end{aligned} \tag{6}$$

In the traditional semi-empirical analysis the radial matrix element $\langle r^{-3}\rangle$ is calculated from the experimental value of the fine structure (fs) splitting $\delta\nu^{\mathrm{fs}}$ by the relation

$$\begin{aligned} &\langle r^{-3}\rangle^{\mathrm{fs}}_{n,l}\,F_j(Z_i) = \\ &= \delta\nu^{\mathrm{fs}}/[a_0^3\,R_\infty\,\alpha^2(l+1/2)\,Z_i\,H_r(l, Z_i)/F_j(Z_i)]. \end{aligned} \tag{7}$$

The ratio of the relativistic correction factors $Z_i\,H_r(l, Z_i)/F_j(Z_i)$ has been calculated by Schwartz [22] and is found to be 106.6 for the $7p\,^2P_{3/2}$ state in Ra II. With $\delta\nu^{\mathrm{fs}}=4857.66\ \mathrm{cm}^{-1}$ for the $7p$ doublet one obtains $\langle r^{-3}\rangle_{7p_{3/2}}\,F_{3/2}=5.199\,a_0^{-3}$. This semi-empirical analysis of the magnetic hfs yields the values for $H_e(0)$ as given in Table 3. They are 15% smaller than the experimental values that one calculates directly from the independently measured A-factors and μ_I values.

An alternative semi-empirical access to the radial integral is given by the Goudsmit-Fermi-Segrè formula, which makes use of the quantum defect theory

Table 3. Magnetic hyperfine fields $H_e(0)$ in units of Tesla. The experimental values (Column 2) are compared with the results from the semi-empirical analysis of the fine structure (Column 3), the Goudsmit-Fermi-Segrè (GFS) formula (Column 4) and the RMBPT calculations (Column 5)

State	$H_e(0)(T)$ Exp.	fs	GFS	RMBPT
$7p\,^2P_{1/2}$	242.3[a]	196.6[b]	226[b]	243[c] 246[d]
$7p\,^2P_{3/2}$	62.5[a]	52.6[b]	57.7[b]	63.1[c] 64.6[d]

[a] Ref. [3], [b] This work, [c] Ref. [4], [d] Ref. [5]

in order to normalize the electronic wave function near the origin. It reproduces within a few percent the hyperfine field of the Ra II ground state [1, 2] as in all cases of $^2S_{1/2}$ states known. For the $7p$ doublet, however, it yields again numbers 7–8% below the experimental value (cf. also [2]). On the other hand, ab initio calculations of $H_e(0)$, using relativistic many-body perturbation theory (RMBPT) [4, 5] meet the experimental values quite well (see Table 3). A closer inspection of these calculations reveals that core polarization, from which the contact term in (2) arises, as well as correlation effects, extrapolated from similar atomic systems in [5], contribute quite significantly to the magnetic hfs. This may explain why the semi-empirical evaluation of the direct valence contribution to $H_e(0)$ does not exhaust the experimental value. A similar discrepancy of 18% is found in francium [23], whereas in the p-doublets of the lighter alkali and alkali-like spectra the semi-empirical $H_e(0)$, corrected for core polarization, accounts for 95–100% of the experimentally observed value (the scatter arising from different choices of relativistic corrections is included in this interval).

4.2. *Analysis of the quadrupole splitting*

The problem of evaluating the electric field gradient in radium was circumvented in the preliminary results of Ahmad et al. [1] by the assumption that for well-deformed nuclei around ^{228}Ra the spectroscopic quadrupole moments Q_s can be safely related to the intrinsic ones Q_0 by the strong-coupling projection formula. The intrinsic quadrupole moments for the doubly-even isotopes are known from the $B(E2)$ values of nuclear spectroscopy. This procedure yielded the value $Q_s(^{229}\mathrm{Ra})=2.9$ b and thus provided an effective calibration of $\phi_{zz}(0)$ for all B-factors measured. In a second paper [2], a first semi-empirical evaluation of electric field gradients in Ra was given based on a systematic analysis of the $7s\,7p\,^3P_J$ configuration in Ra I yielding $Q_s(^{229}\mathrm{Ra})=2.9$ b in good agreement with the previous value.

The alkali-like spectrum of the radium ion is expected to provide a more reliable access to the spectroscopic quadrupole moments owing to its simplicity. In this case, the relation between the B-factor and Q_s is explicitly given by [18]

$$Q_s=(4\pi\varepsilon_0/e^2)\,[(2j+2)/(2j-1)] \cdot(1/R_{lj}(Z_i))\,(1/\langle r^{-3}\rangle_{nl})\,B/(1-R), \tag{8}$$

where $R_{lj}(Z_i)$ is a relativistic correction factor for the radial quadrupole matrix element. It can be deduced again from $\delta\nu^{\mathrm{fs}}$ using the relation [18]

$$R_{lj}\langle r^{-3}\rangle^{\mathrm{fs}}_{nl}= =\delta\nu^{\mathrm{fs}}/[a_0^3\,R_\infty\,\alpha^2(l+1/2)\,Z_i\,H_r(l,Z_i)/R_{lj}]. \tag{9}$$

With $Z_i H_r(l,Z_i)/R_{p_{3/2}}=90.6$ from [22] we obtain $R_{p_{3/2}}\langle r^{-3}\rangle_{7p_{3/2}}=6.116\,a_0^{-3}$. Adopting further a Sternheimer correction factor $(1-R)=1.20(4)$ [24] the semi-empirical analysis of the B-factor in the $7p\,^2P_{3/2}$ state of Ra II yields the spectroscopic quadrupole moments $Q_s(^{221}\mathrm{Ra})=1.978(7)$b and $Q_s(^{223}\mathrm{Ra})=1.254(3)$b, where the errors bars reflect so far only the experimental uncertainties of the B-factors.

An alternative, occasionally used way to deduce the radial matrix element is based on the magnetic hfs coupling. By inserting experimental μ_I-values as well as a-factors, corrected for core polarization, into (3) the quantity $F_j(Z_i)\langle r^{-3}\rangle_{nl}$ is obtained. According to Sect. 4.1, this procedure results in a radial matrix element 15% larger than that derived from the fs splitting. Obviously, one should not use this approach in the case of Ra II, since the A_p-factors seem to contain higher-order contributions which are difficult to disentangle within the semi-empirical analysis of Sect. 4.1.

The analysis of the hfs in the $7s\,7p$ configuration of Ra I [2] yields Q_s values in good agreement with the ones given in the present work (see Table 4). In

Table 4. Compilation of Q_s-values in units of 10^{-24} cm^2 (barn). Columns 2 and 4 give the results from the semi-empirical analysis of the fs in Ra II and Ra I [2], respectively. The B/Q ratio obtained from the RMBPT calculation [5] together with the measured B-factors yields the values given in column 3. The errors including estimated general scaling uncertainties are given in the second brackets. Ratios of quadrupole moments are accurate within the experimental errors

	Q_s(b)			
A	fs Ra II	RMBPT	fs Ra I	$B(E2)$
221	1.978 (7) {106}[a]	2.02[b]	1.907 (7) {198}[c]	1.9[d]
223	1.254 (3) {66}[a]	1.28[b]	1.190 (7) {126}[c]	1.2[d]

[a] This work, [b] Ref. [5], B-factors taken from this work
[c] Ref. [2], [d] Ref. [1]

Table 5. Final Q_s values for all isotopes measured so far (in units of barn). $Q_s(^{221}\mathrm{Ra})$ and $Q_s(^{223}\mathrm{Ra})$ directly from the hfs analysis of Ra II (see Table 4, Column 2). These results in combination with the B-factors of Ref. [2] are used to recalculate the quadrupole moments of the other isotopes. For errors see Table 4

A	209	211	221	223	227	229
$Q_s(b)$	0.40 (2) {4}	0.48 (2) {4}	1.978 (7) {106}	1.254 (3) {66}	1.58 (3) {11}	3.09 (4) {19}

that case $\langle r^{-3}\rangle$ was also derived from $\delta\nu^{\mathrm{fs}}$. According to [25] ab initio calculations of ϕ_{zz} seem to favour quite generally a semi-empirical analysis of $\langle r^{-3}\rangle$ based on the fs rather than on the magnetic hfs.

The results obtained from the Ra II spectrum are supported by a recent RMBPT calculation of the field gradient, which includes core polarization and empirically estimated correlation effects (see also Sect. 4.1). For the $7p\,^2P_{3/2}$ state of Ra II Heully et al. [5] quote the ratio $B/Q=674.1$ MHz/b. Using the experimental B-factor one calculates $Q_s(^{221}\mathrm{Ra})=2.02$ b.

The results of the four different evaluations of Q_s values are listed in Table 4 for the two isotopes ^{221}Ra and ^{223}Ra investigated in this work. Although one observes satisfactory agreement between all four evaluations, we regard those stemming from Ra II as being the most reliable ones. The values of Q_s for the other isotopes, listed in Table 5, are obtained by multiplying the semi-empirical value based on the fs splitting with the ratios of the B-factors from [2]. We note that with a different choice of relativistic corrections the results may change by a few percent (cf. [18, 21]). Considering the freedom in the choice of relativistic correction factors, the error estimate for the Sternheimer correction, and the general systematics of differently evaluated electric field gradients ϕ_{zz}, we adopt a total calibration error of $\pm 5\%$ for the present semi-empirical analysis in Ra II (as compared to $\pm 10\%$ chosen for the Ra I analysis in [2]).

5. The J-dependence of the isotope shift

The IS between two isotopes with masses A and A' in an optical transition i is described in general by the sum of the field shift $\delta\nu_{f,i}$ and the mass shift $\delta\nu_{m,i}$

$$\delta\nu_i^{A,A'}=\delta\nu_{f,i}+\delta\nu_{m,i}$$
$$=F_i\,\lambda^{A,A'}+(A'-A)/(AA')\,(N_i+S_i). \qquad (10)$$

Here $\delta\nu_{m,i}$ is again the sum of the normal mass shift, described by the constant $N_i=\nu_i/1836.15$ according to the reduced mass of the system, and the specific mass shift described by the constant S_i. The latter is due to the correlation of the electron momenta and therefore difficult to calculate. The field shift is usually factorized into an electronic part, given by the electronic factor F_i and a nuclear part $\lambda^{A,A'}$ (see, for example [26]). The electronic factor F_i is proportional to the change of the electronic charge density at the nucleus $\Delta|\psi(0)|^2$ occurring in the transition. F-factor ratios for different transitions i, j can be obtained from a King plot [27], which yields a straight line with the slope $\kappa=F_i/F_j$ and the intercept with the ordinate $(S_i-S_jF_i/F_j)$. Figure 3 shows the King plot of the transition $7s\,^2S_{1/2}-7p\,^2P_{1/2}$ ($\lambda=468.3$ nm) against the transition $7s\,^2S_{1/2}-7p\,^2P_{3/2}$ ($\lambda=381.4$ nm) in Ra II. The insets, magnified by a factor of 100, show the consistency of the data. The straight-line fit yields a slope of $\kappa=0.9343(6)$ and the intercept $-54(54)$ GHz. The slope of the straight line should be unity, if both the $p_{1/2}$- and the $p_{3/2}$-electron had a vanishing charge density at $r=0$ and their screening factors (cf. [28, 29]) were the same. Assuming the latter statement

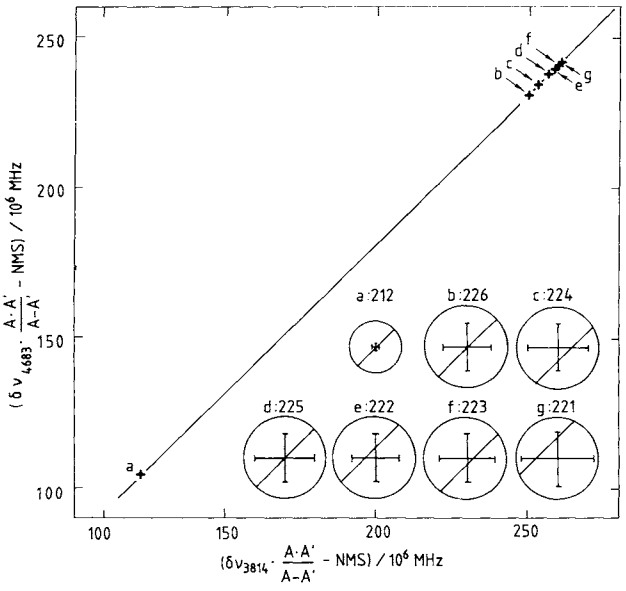

Fig. 3. King plot of IS values (minus the normal mass shift (NMS)) in the Ra II $7p$ doublet with $\lambda=381.4$ nm and $\lambda=468.3$ nm, related to the reference isotope ^{214}Ra. The insets, magnified by a factor of 100, show the excellent consistency of the data

to hold, the difference $\zeta=(1-\kappa)=6.57(6)\%$ can be ascribed to the relativistic enhancement of the $p_{1/2}$ electron wave function at the origin. Following the semi-empirical formula discussed first in the case of Ba II [10], and later modified by Bauche et al. [28], ζ is given by

$$\zeta=|\psi_{p_{1/2}}(0)|^2/|\psi_{s_{1/2}}(0)|^2= \\ =\frac{\alpha^2Z^2}{(1+\sqrt{1-\alpha^2Z^2})}\frac{Z_i(p_{1/2})^2}{Z_i(s_{1/2})^2} \\ \cdot\left(\frac{T(p_{1/2})}{T(p_{3/2})}\right)^{3/2}\frac{1}{(1-\mathrm{d}\sigma/\mathrm{d}n)_{s_{1/2}}}. \quad (11)$$

With the commonly used effective charges $Z_i(p_{1/2})=Z-4$, $Z_i(s_{1/2})=Z$ and $(1-\mathrm{d}\sigma/\mathrm{d}n)_{s_{1/2}}=1.12$ one obtains $\zeta=6.8\%$, in good agreement with the experimental value. Since this analysis was also successful in the cases of the Ba II and Fr I doublets [23] it can now be regarded as being established.

The electronic factors for Ra II in the investigated transitions were caculated by Torbohm et al. using an ab initio Dirac-Fock method [29] with the result $F(468.3)=-39.460\,\mathrm{GHz/fm^2}$ and $F(381.4)=-41.976\,\mathrm{GHz/fm^2}$. The ratio $F(468.3)/F(381.4)=0.940$ can be compared directly with the slope resulting from the King plot. Irrespective of the absolute accuracy of the electronic factors, the good agreement of theoretical ratio with the experimental result confirms the general finding that field shift ratios are very well reproduced by ab initio calculations.

6. Conclusion

The present work completes our investigations on hfs and IS in the Ra I and Ra II spectra [1–3]. The semi-empirical calculation of the hyperfine fields in the $7p$ doublet of Ra II, based on its fs splitting, accounts for only 85% of the experimentally observed magnetic hyperfine fields, whereas ab initio RMBPT calculations meet the experimental values. In the case of the electric field gradient the semi-empirical analysis coincides with the ab initio calculation, corrected empirically for correlation effects. Applied to the B-factors of Ra II this gives more reliable values of spectroscopic quadrupole moments in the series of Ra isotopes. The comparison of the IS in both transitions connecting the ground state with the first excited doublet in Ra II shows the influence of the relativistic $p_{1/2}$-electron charge density at the nucleus as has already been observed in the spectra of Ba II and Fr I.

The authors are grateful to Prof. T.P. Das for various discussions on theoretical problems. We would like to thank Prof. R.M. Sternheimer for the calculation of the Sternheimer correction factor. This work has been funded by the German Federal Minister for Research and Technology (BMFT) under the contract number 06 Mz 458I and the Deutsche Forschungsgemeinschaft (DFG).

References

1. Ahmad, S.A., Klempt, W., Neugart, R., Otten, E.W., Wendt, K., Ekström, C.: Phys. Lett. **133**B, 47 (1983)
2. Wendt, K., Ahmad, S.A., Klempt, W., Neugart, R., Otten, E.W., Stroke, H.H.: Z. Phys. D – Atoms, Molecules and Clusters **4**, 227 (1987)
3. Arnold, E., Borchers, W., Carré, M., Duong, H.T., Juncar, P., Lermé, J., Liberman, S., Neu, W., Neugart, R., Otten, E.W., Pellarin, M., Pinard, J., Ulm, G., Vialle, J.L., Wendt, K.: Phys. Rev. Lett. **59**, 771 (1987)
4. Dzuba, V.A., Flambaum, V.V., Sushkov, O.P.: Phys. Scr. **32**, 507 (1985)
5. Heully, J.L., Mårtensson-Pendrill, A.M.: Phys. Scr. **31**, 169 (1985)
6. Das, T.P.: Private communication; (to be published)
7. Ahmad, S.A., Klempt, W., Neugart, R., Otten, E.W., Reinhard, P.-G., Ulm, G., Wendt, K.: Nucl. Phys. A**483**, 244 (1988)
8. Ravn, H.L., Bjornstad, T., Hoff, P., Jonsson, O.C., Kugler, E., Sundell, S., Vosicki, B.: Nucl. Instrum. Methods B**26**, 183 (1987)
9. Mueller, A.C., Buchinger, F., Klempt, W., Otten, E.W., Neugart, R., Ekström, C., Heinemeier, J.: Nucl. Phys. A**403**, 234 (1983)
10. Wendt, K., Ahmad, S.A., Buchinger, F., Mueller, A.C., Neugart, R., Otten, E.W.: Z. Phys. A – Atoms and Nuclei **318**, 125 (1984)
11. Neugart, R.: Collinear fast-beam laser spectroscopy. In: Progress in atomic spectroscopy. Part D. Beyer, H.-J., Kleinpoppen, H. (eds.). New York: Plenum Press 1987
12. Neugart, R., Stroke, H.H., Ahmad, S.A., Duong, H.T., Ravn, H.L., Wendt, K.: Phys. Rev. Lett. **55**, 1559 (1985)
13. Hänsch, T.W., Couillaud, B.: Opt. Commun. **35**, 444 (1980)
14. Nash, F.R., Bergman, J.G., Boyd, G.D., Turner, E.H.: J. Appl. Phys. **40**, 5201 (1969)
15. Nath, G., Haussühl, S.: Appl. Phys. Lett. **14**, 154 (1969)
16. Neu, W., Passler, G., Sawatzky, G., Winkler, R., Kluge, H.-J.: Z. Phys. D – Atoms, Molecules and Clusters **7**, 193 (1987)
17. Renn, A., Hese, A., Büsener, H.: Laser Optoelektron. **3**, 11 (1982)
18. Kopfermann, H.: Nuclear moments. New York: Academic Press 1958
19. Sternheimer, R.M.: Phys. Rev. **80**, 102 (1950); 146, 140 (1966)
20. Sandars, P.J.H., Beck, J.: Proc. R. Soc. (London) A**289**, 97 (1965)
21. Lindgren, I., Rosén, A.: Case Stud. At. Phys. **4**, 93 (1974)
22. Schwartz, C.: Phys. Rev. **97**, 380 (1955); **105**, 173 (1957)
23. Bauche, J., Duong, H.T., Juncar, P., Liberman, S., Pinard, J., Coc, A., Thibault, C., Touchard, F., Lermé, J., Vialle, J.L., Büttgenbach, S., Mueller, A.C., Pesnelle, A.: J. Phys. B: At. Mol. Phys. **19**, L 593 (1986)
24. Sternheimer, R.M.: Private communication
25. Rosén, A., Lindgren, I.: Phys. Scr. **6**, 109 (1972)
26. Heilig, K., Steudel, A.: At. Data Nucl. Data Tables **14**, 613 (1974)
27. King, W.H.: Isotope shifts in atomic spectra. New York, London: Plenum Press 1984
28. Bauche, J., Büttgenbach, S., Coc, A., Duong, H.T., Juncar, P., Lermé, J., Liberman, S., Mueller, A.C., Pesnelle, A., Pinard, J., Thibault, C., Touchard, F., Vialle, J.L.: J. Phys. (Paris) **47**, 1903 (1986)
29. Torbohm, G., Fricke, B., Rosén, A.: Phys. Rev. A**31**, 2038 (1985)